Synthesis of Planar, Compliant Four-Bar Mechanisms for Compliant-Segment Motion Generation

L. Saggere
Research Fellow,
Mem. ASME

S. Kota
Professor,
Mem. ASME

Department of Mechanical Engineering
and Applied Mechanics,
University of Michigan,
Ann Arbor, MI 48109

Compliant four-bar mechanisms treated in previous works consisted of at least one rigid moving link, and such mechanisms synthesized for motion generation tasks have always comprised a rigid coupler link, bearing with the conventional definition of motion generation for rigid-link mechanisms. This paper introduces a new task called compliant-segment motion generation where the coupler is a flexible segment and requires a prescribed shape change along with a rigid-body motion. The paper presents a systematic procedure for synthesis of single-loop compliant mechanisms with no moving rigid-links for compliant-segment motion generation task. Such compliant mechanisms have potential applications in adaptive structures. The synthesis method presented involves an atypical inverse elastica problem that is not reported in the literature. This inverse problem is solved by extending the loop-closure equation used in the synthesis of rigid-links to the flexible segments, and then combining it with elastic equilibrium equation in an optimization scheme. The method is illustrated by a numerical example.
[DOI: 10.1115/1.1416149]

1 Introduction

By and large, kinematic chains of mechanisms have traditionally been designed to comprise of links that behave as ''rigid'' members. Such mechanisms derive their mobility entirely from rigid-body translations and/or rotations of links due to degrees-of-freedom (DOF) permitted at the kinematic pairs or connections between various links. Elastic deformations of materials have also been utilized to generate useful motions in numerous mechanisms for certain special advantages, but until mid-1960s such flexure generated mobility was largely confined to small angular rotations between stiff members by means of flexure hinge—a short and thin metallic strip or a small ''necked'' down region of a thick blank of material—that provides a rotational DOF similar to that at a conventional pin joint [1]. As opposed to such flexure at joints, generating mobility through elastic deformations of links by replacing one or more links in a conventional kinematic chain with slender flexible members was first suggested by Burns and Crossley [2], and this resulted in a special class of mechanisms called *flexible link mechanisms*. Early works on flexible link mechanisms consisted of four-bar chains consisting one or two flexible members. Since the late 1980s the scope of mechanisms utilizing flexure has broadened tremendously embracing mechanisms with a variety of complex topologies. Today, all mechanisms that are designed to derive mobility from elastic deformations in some element(s)—a flexural hinge and/or a relatively long flexible segment—of a mechanism have come to be broadly referred to as *compliant mechanisms*. For more information on the background of compliant mechanisms interested readers may refer Midha [3], Ananthasuresh [4], and Saggere [5].

This paper concerns a class of compliant mechanisms featuring a closed-loop kinematic chain, i.e., a four-bar, and synthesized for one of the three conventional tasks viz. path, function, or motion generation. This class of mechanisms was first investigated by Burns and Crossley [2]. They approximated the motion of the tip of a flexible cantilever strip as equivalent to the rotation of a rigid-link that is five-sixth of the length of the flexible segment, and based on this approximation, they presented a graphical technique for synthesis of a function generating four-bar linkage with a flexible coupler link. Sevak and McLarnan [6] presented an optimization method based on iterative finite-element analysis technique for synthesis of flexible mechanisms with one or two flexible links in a four-bar chain for function and path generation tasks. Howell and Midha [7] developed a technique called pseudo-rigid-body model wherein a compliant mechanism is modeled as an equivalent rigid-link mechanism, and used this technique to synthesize four-bar compliant mechanisms containing a rigid input link, a rigid coupler and a flexible link for motion generation task. In all of these works, two characteristics are prominent: compliant four-bar mechanisms comprised at least one moving rigid-link, and in compliant mechanisms for motion generation, the coupler link was always considered to be a rigid member. This is because, these works considered the motion generation objective that is based on the definition of the task provided for conventional rigid-link mechanisms. In this paper, we consider a new objective involving the guidance of a slender flexible segment rather than a rigid link, and present a technique to synthesize a single-link compliant mechanism to accomplish the objective task. In what follows, we first outline the problem statement and follow it by a detailed explanation of the synthesis technique. Lastly, we illustrate the synthesis approach by means of a numerical example.

2 Problem Statement

Motion generation is one of the three customary *tasks* for kinematic synthesis of rigid-link mechanisms. Erdman and Sandor [8] have defined it is as the *task* which requires that an entire (rigid) body be guided through a prescribed motion sequence. The ''body'' to be guided is usually a part of a rigid floating link, and the prescribed ''rigid-body motion sequence'' comprises of desired positions and orientations of the floating link. However, if the body to be guided is flexible, then it would undergo elastic deformation in addition to rigid-body motion. Such a case has not been treated so far, and we consider the same in this paper.

Contributed by the Mechanisms Committee for publication in the JOURNAL OF MECHANICAL DESIGN. Manuscript received April 1999. Associate Editor: C. M. Gosselin.

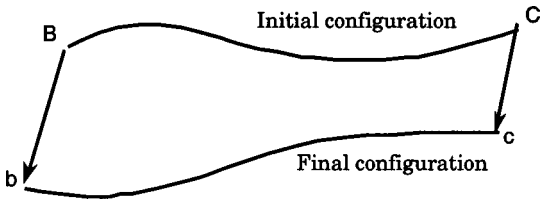

Fig. 1 Illustration of the compliant-segment motion generation task

The objective of the synthesis presented in this paper is to guide a given slender flexible segment with known initial shape, elastic properties, and external loading, if any, to another prescribed configuration. That is, the given flexible segment is to be deformed into another specified definite smooth shape while moving it from its initial configuration to another specified configuration as illustrated in Fig. 1. Such a motion of the segment involves a rigid-body displacement of the segment along with a controlled elastic deformation or change in the shape of the segment. We call such a task of accomplishing such a motion as ''compliant-segment motion generation,'' and, in general, this task could include multiple prescribed configurations (i.e., positions and shapes) of the segment, just as in the case of conventional ''rigid-body motion generation'' task. Thus, compliant-segment motion generation task is *a task that requires a flexible segment of a mechanism to be guided through a sequence of discrete prescribed "shapes," or "precision shapes*.''

Many potential applications of compliant-segment motion generation can be envisioned. For instance, a certain segment of a large flexible space structure that functions as a reflective surface may be required to be oriented in different directions and also shaped into different curvatures for the purposes of modulating the characteristics of reflecting sound or light waves. A similar application of compliant-segment motion generation is also practicable at micro level, for example, in micromirrors for controlled reflection of light. Another example of potential application of compliant-segment motion generation is a stamping application where a flexible contour is required to conform to contoured rigid surfaces that have differently shaped curvatures. In all such applications, the required task can be efficiently accomplished by devising a suitable compliant four-bar mechanism.

To accomplish compliant-segment motion generation, we consider a compliant four-bar topology wherein the two ends of the segment are connected to the ends of two other flexible segments (to be synthesized) so that the three segments form one continuous planar link. The two free ends the link are pinned to ground and actuated by input torques or rotations as shown in Fig. 2. Such a topology may also be referred to as a structurally binary link with three compound segments in the nomenclature suggested by Midha et al. [9]. In this figure, B-C is the given flexible segment to be guided to the specified final configuration b-c; A-B and C-D

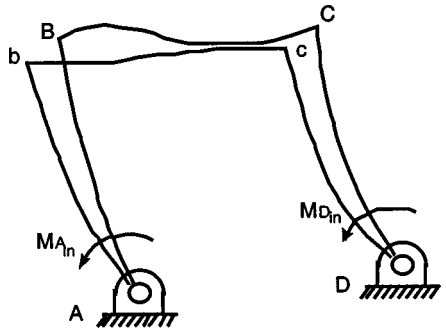

Fig. 2 Complaint four-bar mechanism for motion generation

are two segments to be synthesized; A-B-C-D represents the initial configuration of the mechanism, and A-b-c-D represents the final configuration of the mechanism. Based on the consideration of this topology, the problem statement may be explicitly phrased as follows: *given the initial configuration of a flexible segment and its desired final configuration, synthesize a compliant four-bar mechanism comprising all flexible segments and the corresponding input torques that precisely effect the prescribed compliant-segment motion generation*.

We assume that the specified initial and final shapes of the given flexible segment are ''smooth,'' and can be adequately represented by second or third order polynomials. We also assume that the involved shape change is ''small,'' which means the displacements and strains are ''small'' enough for the application of linearized beam theory, and the beams are ''slender'' so that axial and shear strains are negligible.

3 Synthesis Procedure

The basic goal of the synthesis for compliant-segment motion generation can be separated into two components: the elastic deformation and the rigid-body displacement of the segment. The first component necessitates an appropriate moment distribution over the given flexible segment the second component necessitates appropriate kinematic displacements of the two ends of the segments. Since the geometry of the shape change involved can be represented by either a cubic or a quadratic equation, it is apparent from the Euler's elastic curve equation (which relates the bending moment distribution on a segment to its curvature), that the order of the moment distribution function on the segment has to be at most one. That is, in order to effect quadratic or cubic shape changes, it is sufficient to generate a linearly varying or constant moment distribution along the length of the segment, and this in turn can be accomplished by means of only two unequal or equal end-moments at the two ends of the segment. Based on this fundamental concept, the synthesis strategy aims to accomplish both the required moment distribution (end-moments) on the given segment and the prescribed kinematic displacements of its two ends by appropriately synthesizing the two segments pinned to the ground and the corresponding input moments. Thus, specifically, the synthesis tasks are: to determine optimal shapes and sizes of segments A-B and C-D, locations of the pivots A and D, and the input torques MA_{in} and MD_{in} of the compliant mechanism in Fig. 2.

The approach adopted for this synthesis is conceptually similar to that of rigid-link four-bar mechanisms in that it involves disjoining the mechanism into various links and designing each link separately, however, its implementation is very much modified in view of the fact that pure kinematic motion and elastic deformations cannot be treated separately in compliant mechanisms. The synthesis strategy is to disjoin all the segments and impose boundary conditions on each segment so that (a) at the fusing ends, displacements and rotations are identical and the internal forces and moments are equal in magnitude but opposite in sign, and (b) each segment is independently in equilibrium. These two conditions ensure that when the segments are joined, (a) all the internal forces and moments cancel each other, (b) displacements and rotations are *compatible* at the fusing ends, and (c) the resulting structure will be in equilibrium under the action of input actuation moments. This approach is illustrated in Fig. 3.

This process of setting up of boundary conditions begins with determination of forces and moments as well as corresponding rotations at the ends ''B'' and ''C'' of the coupler segment ''B-C'' that is to be guided. These loads and the prescribed kinematic displacements of the ends ''B'' and ''C'' are translated into boundary conditions for the two input segments ''A-B'' and ''C-D.'' Thus, the synthesis strategy can be divided into two main steps: computation of end-loads on the coupler segment, and synthesis of the input segments.

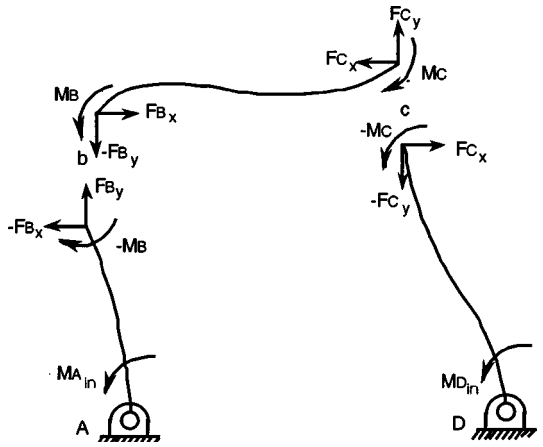

Fig. 3 Boundary conditions set-up for dimensional synthesis of the segments

3.1 Computation of End-Loads on the Coupler Segment. The loads (forces and moments) at the ends of the floating segment corresponding to the desired shape change in the segment are determined by a standard method of mechanics. For this purpose, the rotations at the ends are first calculated from the equations of the known initial and final (deformed) configurations; then, the moments corresponding to the end rotations are computed using the basic slope-deflection equation of the moment distribution method in structural analysis [10]. Since the slope-deflection equation of the moment distribution method is not commonly used in modern structural analysis literature, its derivation, taken from [10], is presented below for the benefit of the readers.

For ease of illustration of the method, and without any loss of generality, let the initial shape of the member be straight. Figure 4 represents the deflected shape n-f of a straight member N-F. Clockwise moment or rotation of either end of the member is considered positive. The relative translation of the ends perpendicular to the original direction of the member, $(y_F - y_N)$, produces bending and the relative translation along the axis of the member, x, is considered to be zero, that is, it is considered that no change in length occurs. The chord rotation, $\varphi = (y_F - y_N)/l$, is considered positive when clockwise. Further notation is as follows:

- α_N = rotation at the end N (near end)
- α_F = rotation at the end F (far end)
- S_N = rotational stiffness of end N—that is, the end-moment at N corresponding to a unit rotation at N while the displacement at F is restrained. (Fig. 4-*b*)
- S_F = rotational stiffness of end F—that is, the end-moment at F corresponding to a unit rotation at F while the displacement at N is restrained. (Fig. 4-*c*)
- t = carry-over moment—that is, the moment at the fixed end F caused by a unit rotation of end N (Fig. 4-*b*); also equal to the carry-over moment at the fixed end N caused by a unit rotation of end F (Fig. 4-*c*) (by Betti's theorem).

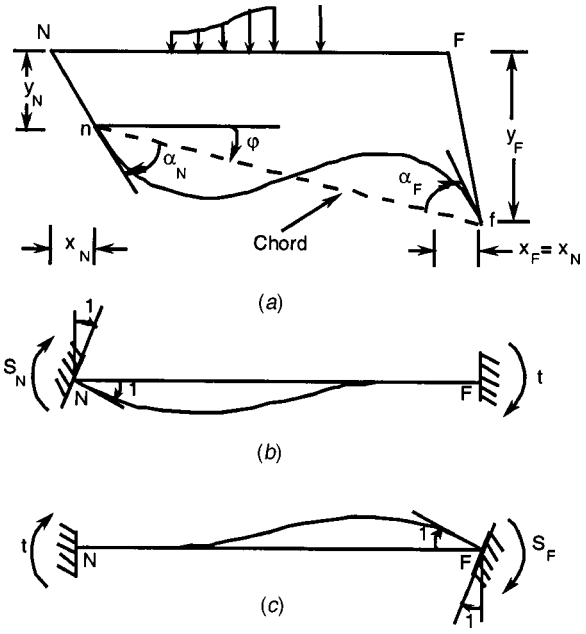

Fig. 4 Sign convention for slope-deflection equation. (a) Positive directions of end-rotations α_N and α_F, and chord rotation φ. (b) End-moments caused by a unit rotation at N. (c) End-moments caused by a unit rotation at F.

Consider the curve n-f representing the deformed shape of a member N-F subjected to external lateral loads (Fig. 4-*a*). The translation part of the displacement of the member (that is, its translation as a rigid-body to the straight dotted line n-f) produces no moments. The end-moment M_N at end N can be expressed as the sum of the moment due to the external load on the member with the end-displacements prevented (the fixed-end moment M_{ext}) and of the moments induced by rotations $(\alpha_N - \varphi)$ and $(\alpha_F - \varphi)$ at the ends N and F respectively. Thus, $M_N = S_N(\alpha_N - \varphi) + t(\alpha_F - \varphi) + (M_{ext})_N$ where $(M_{ext})_N$ is the fixed end-moment at N, that is, the value of the end-moment caused by the actual external lateral loads on the beam with displacements at both ends prevented. This equation can be rearranged as $M_N = S_N\alpha_N + t\alpha_F - \varphi(S_N + t) + (M_{ext})_N$. This is the slope-deflection equation for a prismatic or non-prismatic beam. The equation can be used to express the moment at the left- or right-hand end. When the member has a constant flexural rigidity EI, $S_B = 4EI/l$ and $t = 2EI/l$. The slope-deflection equation then becomes:

$$M_N = \frac{EI}{L}(4\alpha_N + 2\alpha_F - 6\varphi) + (M_{ext})_N \tag{1}$$

Using this slope-moment equation, moments required at the ends B and C of the segment B-C in Fig. 3 are determined. Once the end-moments have been established, the forces required for the equilibrium of the segment at each of the two ends are determined from simple statics, and then, the computed force at each end may be resolved into horizontal and vertical components through the known angle of orientation of the chord with respect to the horizontal.

3.2 Synthesis of Input Segments. This synthesis process begins with setting up the right boundary conditions on the segments. With reference to Fig. 3, the boundary conditions on the segments A-B and C-D are set-up as follows: the forces and moments determined at the ends B and C of segment B-C are transferred to the ends B and C of the segments A-B and C-D as explained earlier; the rotations required at the ends B and C are computed from the known change in curvature of the segment B-C; and the displacements of the ends B and C are known directly from the design specifications. The rotations and input moments at the ends A and D are also part of the boundary conditions for the synthesis, but their values are unknown. After establishing the boundary conditions, the objective of the synthesis is to determine the shapes and sizes of segments A-B and C-D, locations of the pivots A and D, and the unknown values of the input torques MA_{in} and MD_{in} which satisfy the equilibrium of the segments. Since the synthesis process is identical for both the segments A-B and C-D, we consider only one segment in the following.

Consider the segment A-B, for instance. Figure 5 illustrates the known and unknown design parameters involved in the synthesis of segment A-B. The forces F_{B_x}, F_{B_y}, the moment M_B, the displacement d at an angle δ from the horizontal, and the rotation

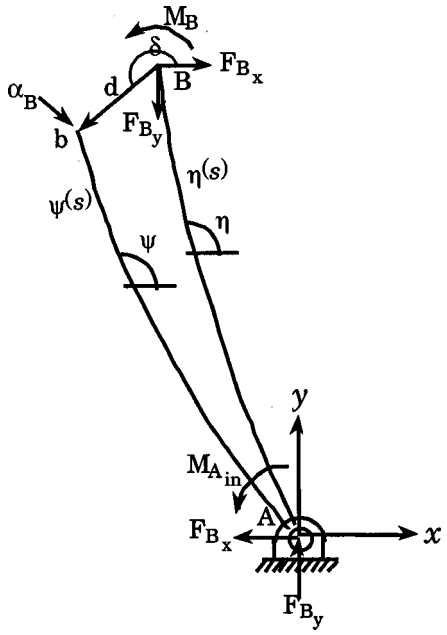

Fig. 5 Design parameters involved in synthesis of the segment A-B

α_B at the tip B—are all known; the unknown quantities are the length and the shape of the segment, the location of the ground point A, and the input moment $M_{A_{in}}$ required at the tip A. All these known and unknown quantities are related through the equilibrium condition for the segment, and constitute and an inverse elastica problem as discussed in the following.

3.2.1 An Atypical Inverse Elastica Problem. The most common problem in the theory of bending is that in which the free shape of a beam with a particular load is given and the deflected shape is sought. This problem is rather straight-forward to solve. If the expected deflections are small, the problem can be easily solved by the Euler-Bernoulli linear beam theory; but in the case of large, non-linear deflections a more sophisticated model such as the *elastica* is necessary. However, in many engineering applications there exist problems which are the inverse of the direct bending problem. One class of such inverse problems involves the case where the length of the beam and locations of its tips and/or tip loads are known, but the equilibrium geometry of the beam is unknown. A problem comprising this particular set of knowns and unknowns in the theory of bending is called the *inverse elastica problem*. Such a problem has been studied by many researchers including Shoup and McLarnan [11], Watson and Wang [12], and Stack et al. [13]. Another class of inverse problems involves the case where the deflected shape of a beam corresponding to a particular load may be given and the free (unloaded) shape of the beam is sought [14]. Excepting the cases where the beam geometry and loads are very simple, such inverse problems have, in general, no closed form solutions, and mostly, they require numerical methods for their solutions. However, as was observed in the works cited, numerical solutions to inverse elastica problems are complicated by the highly non-linear behavior and non-uniqueness of the solutions.

Typically, in such inverse problems either the initial shape or the deformed shape of the beam, the locations of tips of the beam, as well as the total length of the beam are known. However, in the inverse problem under inquiry (problem illustrated in Fig. 5), both the initial shape and the deformed shape are not known, nor are the tip locations and length of the beam known. Further, in this problem, unlike typical inverse problems, both the tip loads and the tip displacements (including rotations) are known. This set of knowns and unknowns in elastic bending theory constitutes a very atypical inverse problem that has not been reported in the literature, and the solvability of this problem is discussed below.

Consider the bending of the curved beam segment in Fig. 5. The shapes of beam's axis in the unloaded (undeformed) and the loaded (deformed) states are planar curves represented by parametric equations $\eta = \eta(s)$ and $\psi = \psi(s)$ respectively, where s is a parameter identified with length measured along the axis of the beam from point A. The beam is assumed to be inextensible, hence s is the same in both equations, and the total arc length of both shapes is L. Thus, $\eta(s)$ and $\psi(s)$ represent the slopes measured with respect to the horizontal, and $\{x_\eta(s), y_\eta(s)\}$ and $\{x_\psi(s), y_\psi(s)\}$ represent the Cartesian coordinates at any point s on the undeformed and the deformed shapes of the beam. It is assumed that one of the principal axes of inertia of the beam's cross-section lies in the plane xy, and the loads acting on it also lie in that plane. Therefore, the axis of the beam remains to be a planar curve after deformation. The required forces and the moment at the tip B are known from the boundary conditions at the end B; this implies that the forces at the end A are also known since they must be equal and opposite to that at B to satisfy the equilibrium condition. However, the input moment $M_{A_{in}}$ is unknown since the relative locations of the tips are not known. Assuming a constant flexural rigidity EI, the in-plane bending of the beam is governed by Euler's equation:

$$EI\frac{d}{ds}\left(\frac{d\psi}{ds}-\frac{d\eta}{ds}\right)=M_{A_{in}}-F_{B_x}y_\psi(s)+F_{B_y}y_\psi(s) \tag{2}$$

and the coordinates $\{x_\eta(s), y_\eta(s)\}$ and $\{x_\psi(s), y_\psi(s)\}$ are related to $\psi(s)$ by the following geometric relations:

$$\frac{dx_\psi(s)}{ds}=\cos(\psi(s)); \quad \frac{dy_\psi(s)}{ds}=\sin(\psi(s))$$

$$\frac{dx_\eta(s)}{ds}=\cos(\eta(s)); \quad \frac{dy_\eta(s)}{ds}=\sin(\eta(s)) \tag{3}$$

The loaded beam is subject to the following displacement boundary conditions at the end B:

$$x_\psi(L)-x_\eta(L)=\int_0^L \cos(\psi(s))-\cos(\eta(s))ds=d\cos(\delta) \tag{4a}$$

$$y_\psi(L)-y_\eta(L)=\int_0^L \sin(\psi(s))-\sin(\eta(s))ds=d\sin(\delta) \tag{4b}$$

$$\psi(L)-\eta(L)=\alpha_B \tag{4c}$$

The above set of non-linear equations forms an under constrained system for the solution of the unknowns EI, $\psi(s)$, $\eta(s)$, $x_\eta(L)$, $y_\eta(L)$, $x_\psi(L)$, $y_\psi(L)$, MA_{in}, and L. One might think of obtaining the loaded shape of the beam segment, $\psi(s)$, by an inverse elastica method, and then solve for $\eta(s)$ in the governing equilibrium Eq. (1). However, expression for $\eta(s)$ obtained by rearranging Eq. (1) has, in general, no closed-form solution. The insufficient information about the beam to be synthesized, or in other words, this set of large number of unknowns poses difficulties even for a solution by numerical methods. The set of unknowns in this system of equations exhibit the existence of infinitely many beam configurations that can satisfy the load-displacement requirements. However, it is possible to obtain uniquely ''best'' possible solutions for such problems by employing constrained optimization techniques. There is no reported work in literature that has particularly treated the above set of knowns and unknowns. One closely related work is that of Banichuck [15], who presented an optimization method for determining the optimal shape of a curved beam loaded by a single concentrated force at the tip of the beam. However, in that problem, the locations of the beam's tips, the length and the total volume of

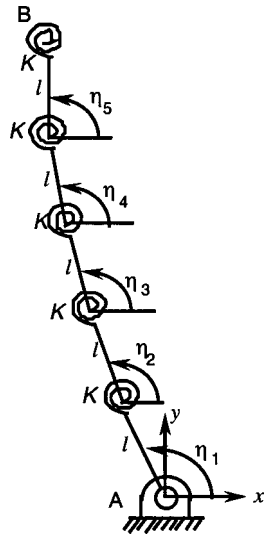

Fig. 6 Model of curved beam using torsional springs and rigid elements

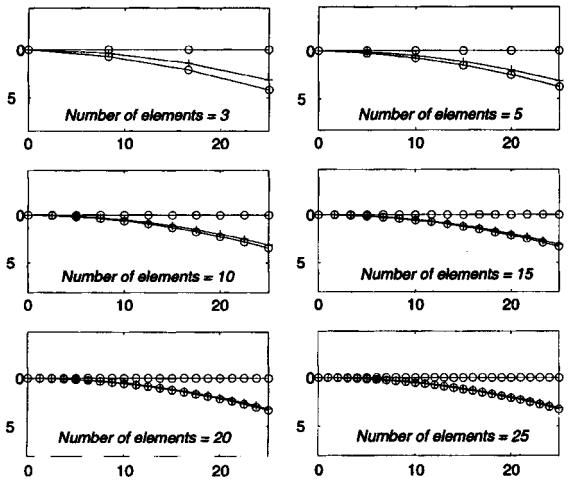

Fig. 7 Comparison of the static deformation of a flexible member using conventional beam elements (-+-) and the spring-model (-0-)

the beam were assumed to be known, and also in that problem the tip deflection was minimized rather than satisfying a specific value of the tip deflection as is the case in the current problem. The difficulty associated with insufficient information for a direct solution to the above set of non-linear equations has been overcome in the following by combining kinematics and mechanics in a novel way through an optimization scheme. Before elucidating the optimization scheme, the details of a model for the beam used in the optimization set-up is in order below.

3.2.2 Modeling a Curved Beam Segment. Since differential equations are cumbersome for optimization by ''classical'' approaches, a method of discretization of the flexible segment into discrete elements is necessary for optimization by a numerical approach. For this purpose, a curved flexible member may be modeled as a series of small, straight, rigid elements connected end to end through linear torsional springs such that the lengths of the rigid elements add up to the length of the original curved beam segment (see Fig. 6). The spring constant, K, of the torsional spring is approximately taken as $K=EI/L$, where EI is the bending stiffness of the beam, and l is the length of the rigid element. Such a model for a curved beam segment characterizes the static deformation behavior of the corresponding beam segment with sufficient accuracy when large number of springs and rigid elements are used in the model. For example, Fig. 7 depicts a comparison of the model with springs and rigid-links with conventional beam elements through a linear analysis for static deformations of a cantilever beam under a moment load at the tip. It can be observed that when fewer elements are used, the spring model predicts larger static displacements (mode -0-) than that predicted by conventional beam elements (mode -+-). However, as the number of elements are increased, the displacement error in the spring model decreases, and the static deformation mode predicted by this model compares better with that of conventional beam elements. This can be explained by the fact that a spring-link element underestimates the bending stiffness of the beam due to the approximation involved in the value of the spring constant. However, as element lengths shorten with increase in number of elements, the approximation error is progressively corrected.

3.3 Optimization. Figure 8 shows the spring-link models of the initial and the final configurations of the beam segment. The angles η_i and ψ_i in Fig. 8 are related to the tip loads, the input actuation (rotation θ_A) and the boundary-conditions through a simple equilibrium equation in terms of spring constant K. To arrive at an optimal feasible solution to the problem, the total weight (or volume) of the segment is minimized as a cost functional subject to the known tip displacement (kinematic constraint) and the known tip rotation (elastic constraint). The design variables and the associated bounds are: $0<l\leqslant l_{\max}$, $0\leqslant\eta_i\leqslant\pi$, $h_{\min}\leqslant h\leqslant h_{\max}$ (cross-sectional width of the member) and $\theta_{\min}\leqslant\theta_A\leqslant\theta_{\max}$ (input rotation at the pinned end A). Thus, the optimization problem is posed as:

$$\begin{aligned} &\textbf{Minimize:} && \text{Volume}=(l\times h^2)\\ &\textbf{Subject to:} && \text{Kinematic Constraint}\\ &&& \text{Elastic Constraint}\\ &&& \text{Equilibrium Equation} \end{aligned} \tag{5}$$

Equilibrium equation: The equilibrium equation is given by:

$$K_i[(\psi_i-\eta_i)-(\psi_{i-1}-\eta_{i-1})]=M_i \quad i=2\ldots n, \tag{6}$$

where M_i is the net moment acting on ith element;

Elastic constraint: This is the required rotation at tip B, that is:

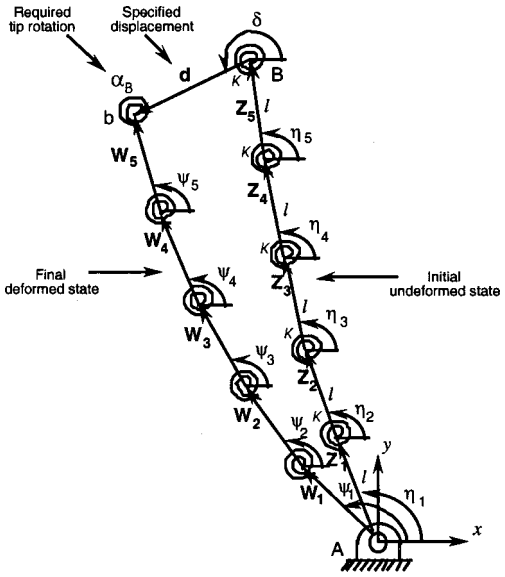

Fig. 8 Notation for the computational scheme of the finite-link model

$$(\psi_n - \eta_n) = \alpha_B ; \tag{7}$$

Kinematic constraint: For the kinematic constraint an idea similar to the standard loop-closure equation employed in the synthesis of traditional rigid-link mechanisms [8] is used. By representing the position of each of the rigid links in its initial and final positions as vectors (see Fig. 8): $\mathbf{Z}_i = l(\cos \eta_i + i \sin \eta_i)$, and $\mathbf{W}_i = l(\cos \psi_i + i \sin \psi_i)$, respectively, and representing the specified tip displacement as vector **d**, a loop-closure equation for the two positions can be written as:

$$\sum_{i=1}^{n} (\mathbf{W}_i - \mathbf{Z}_i) = \mathbf{d} \tag{8}$$

The two scalar components of this vector equation are:

$$l\sum_{i=1}^{n} (\cos \psi_i - \cos \eta_i) = d \cos \delta$$

$$l\sum_{i=1}^{n} (\sin \psi_i - \sin \eta_i) = d \sin \delta \tag{9}$$

where δ is the orientation of the displacement vector **d** as shown in Fig. 8. The optimization is started with initial ''guess'' values for the design variables, and at convergence, it yields a set of optimal values for l, and η_i, $(i = 1..n)$ that defines the shape, the length, the ground pivot of the flexible segment, as well as, the magnitude of the input actuation (moment M_{Ain}, or rotation θ_A). The accuracy with which the converged values will satisfy the synthesis requirements depends on the convergence tolerance set for the optimization and number of the elements employed in the model.

The above steps must be repeated to synthesize the remaining segment C-D. Then, the shapes of all three compliant segments, A-B, B-C, and C-D will be known. The structure that results by connecting the three segments end-to-end and pinning the ends A and D to ground pivots is the required compliant mechanism for the specified task.

4 Example

Consider a 200 mm long flexible beam BC which is initially straight and oriented at 14.47° with respect to a horizontal axis of a Cartesian coordinate system is required to be guided into a new position and bent into a shape where the axis of the beam, identified by a parameter s, is represented by the cubic equation: $-0.8\times10^{-5}s^3 + 0.00235s^2 + 0.1s$ when the end B is at the origin of the Cartesian frame (see Fig. 9). Let the required displacements at the two ends be: $d_b = 10$ mm at an angle $\delta_B = 200°$ and $d_c = 10$ mm at an angle $\delta_C = 200°$. Let the specified properties of the beam be: Young's modulus, $E = 20\times10^4$ N/mm^2, and width of its square cross-section, $h = 5$ mm ($I = 52.08$ mm^4).

First, the required rotations at the ends are computed from the known change in geometry: $\alpha_B = -0.1$ radians and $\alpha_C = -0.08$ radians. The chord rotation and the length of the beam are given, viz. $\varphi = 14.47°$ and $L = 200$ mm, and since no external load is specified on the beam, we have $M_{ext} = 0$. By substituting the known values viz. E, I, l, α_B, α_C, φ, and M_{ext}, in Eq. (1), the necessary end-moments to effect the desired deformation are computed: $M_B = -29166.5$ N-mm, and $M_C = -27083.16$ N-mm. Then, applying the basic moment equilibrium principle from statics, the end-forces at the two ends of the segment BC are obtained, and resolved into horizontal and vertical components in the Cartesian coordinate system: $F_{Bx} = 70.31$ N, $F_{By} = -272.32$ N, and $F_{Cx} = -70.31$ N, $F_{Cy} = 272.32$ N (see Fig. 10).

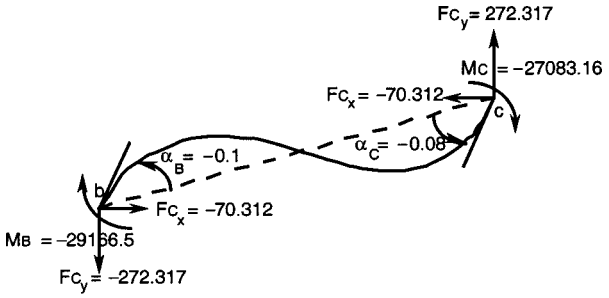

Fig. 10 A schematic illustrating the computed end-moments and end-forces

Next, the compliant segments AB and CD are synthesized by applying the optimization scheme described earlier. Consider the synthesis of segment AB. The compatible loads at the tip B are known from the computation of equilibrium loads for the segment BC and the compatible displacement and rotation at the tip B are known from the problem specifications. That is, the boundary conditions $F_{Bx} = -70.312$ N, $F_{By} = 272.317$ N, and $M_B = 29166.5$ N-mm, $d_{Bx} = -9.3$ mm, $d_{By} = 3.4$ mm, and $\alpha_B = -0.1$ radians are enforced at the tip B. The curved beam with end A pinned to the ground is modeled using spring-link elements as shown in Fig. 8. Choosing the following bounds for the design variables: square cross-section width, $10\text{ mm} \leqslant h \leqslant 50$ mm; length of each element, $0\text{ mm} \leqslant l \leqslant 100$ mm; and initial orientations of the elements, $0 \leqslant \eta_i \leqslant \pi$ radians, the optimization problem was set-up and solved in the MATLAB® software package for various number of elements n in the model. The optimized values of the set $\{l$ and $\eta_i,\ i = 1 \ldots n\}$ were used to construct the shape for segment AB.

Figure 11 illustrates how the above optimization problem converges for various cases of $n = 2$, 5, 10, 15, 20, and 25. In all of these cases the optimum value of h was 10 mm. It can be observed that as the number of the beam elements, n, increases, the shape of the resulting curve becomes progressively smoother. The differ-

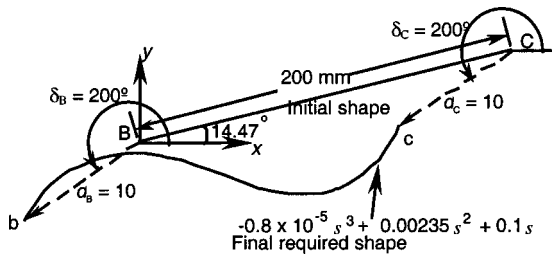

Fig. 9 A schematic illustrating the design specifications

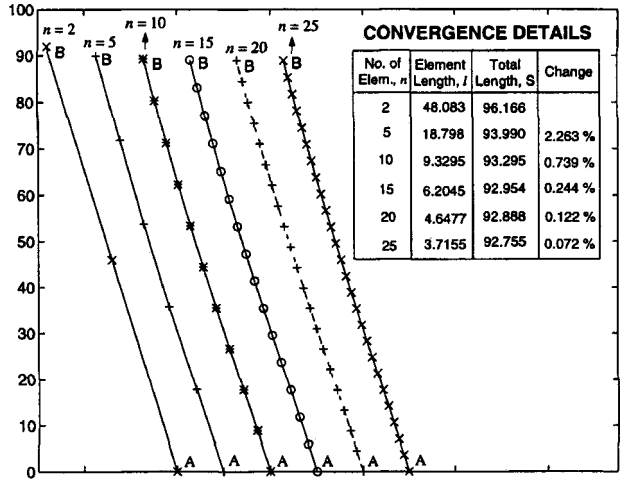

CONVERGENCE DETAILS

No. of Elem., n	Element Length, l	Total Length, S	Change
2	48.083	96.166	
5	18.798	93.990	2.263 %
10	9.3295	93.295	0.739 %
15	6.2045	92.954	0.244 %
20	4.6477	92.888	0.122 %
25	3.7155	92.755	0.072 %

Fig. 11 Results of synthesis of segment AB

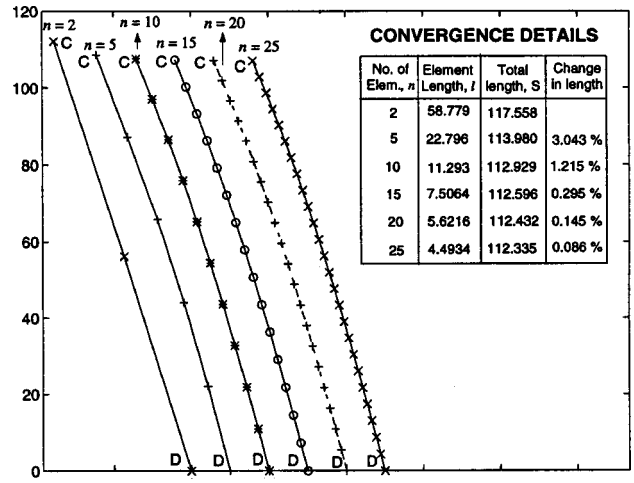

CONVERGENCE DETAILS

No. of Elem., n	Element Length, l	Total length, S	Change in length
2	58.779	117.558	
5	22.796	113.980	3.043 %
10	11.293	112.929	1.215 %
15	7.5064	112.596	0.295 %
20	5.6216	112.432	0.145 %
25	4.4934	112.335	0.086 %

Fig. 12 Results of synthesis of segment CD

ence in the lengths of the beam segment for the cases $n=20$ and $n=25$ was less that 0.1% which was considered as an acceptable tolerance for the convergence.

The synthesis procedure was repeated to synthesize the segment CD. The compatible boundary conditions enforced at the tip C for the optimization are: $F_{Cx}=-70.312$ N, $F_{By}=272.317$ N, and $M_C=27083.16$ N-mm, $d_{Cx}=-9.39$ mm, $d_{Cy}=3.42$ mm, and $\alpha_C=-0.08$ radians. The convergence of the results for this segment is illustrated in Fig. 12. In all of these cases also, the optimum value of h was 10 mm.

After completing the synthesis of the segments AB and CD, these segments are connected to the given segment BC, and the required flexible four-bar mechanism (shown in Fig. 13) is obtained. Finally, having established the relative distance between the ends of each of the segments AB and CD, and as well as the end-forces at B and C, the necessary input moments at ends A and D are computed from static equilibrium to be: $M_A=28085.63$ N-mm and $M_D=28753.94$ N-mm.

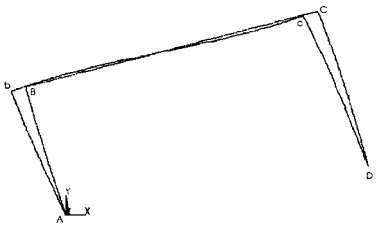

	Tip B		Tip C	
	Specified	FEA	Specified	FEA
Rotation	10 mm	10.1 mm	10 mm	10.05 mm
Displacement	0.1 radians	0.102 radians	0.08 radians	0.081 radians

Fig. 13 Finite element analysis of the resulting complete mechanism after synthesizing the three segments: A-B, B-C, and C-D. (A-B-C-D represents the initial undeformed position of the mechanism, and A-b-c-D represents its final deformed position obtained by a finite-element analysis).

To confirm the synthesis procedure, a finite-element analysis was performed on the resulting compliant mechanism by applying the computed input moments at the pinned ends A and D. The motion of the segment BC, depicted in Fig. 13, was found to conform to the specifications to an accuracy of first decimal.

Conclusions

The problem of effecting a prescribed shape change in a given flexible segment along with its rigid-body motion, called compliant-segment motion generation task, is introduced for the first time, and a first-principles based procedure for synthesis of a closed-loop compliant mechanism for such a task is presented. The procedure is illustrated through a numerical example, and the feasibility of the approach is verified through a reverse finite element analysis. Although motion generation involving only two configurations is considered, the procedure can be extended to motion generation involving multiple configurations.

Acknowledgments

The authors gratefully acknowledge the support provided for this research by the Air-Force Office of Scientific Research under the grant number F49620-96-1-0205.

References

[1] Paros, J. M., and Weisbord, L., "How to Design Flexure Hinges," Machine Design, Nov. 25, 1965, pp. 151–156.
[2] Burns, R. H., and Crossley, F. R. E., 1968, "Kinetostatic Synthesis of Flexible Link Mechanisms," ASME Paper No. 68-MECH-36.
[3] Midha, A., 1993, "Chapter 9: Elastic Mechanisms," *Modern Kinematics—The Developments in the Last Forty Years*, A. G. Erdman (Ed.), John Wiley and Sons Inc.
[4] Ananthasuresh, G. K., 1994, "A New Design Paradigm in Micro-Electromechanical Systems & Investigations on Compliant Mechanisms," Ph.D. Dissertation, University of Michigan.
[5] Saggere, L., 1998, "Static Shape Control of Smart Structures: A New Approach Utilizing Compliant Mechanisms," Ph.D. Dissertation, University of Michigan.
[6] Sevak, N. M., and McLarnan, C. W., 1974, "Optimal Synthesis of Flexible Link Mechanisms with Large Static Deflections," ASME Paper No. 74-DET-83. (Also published in J. Eng. Ind., May 1975, pp. 520–526).
[7] Howell, L. L., and Midha, A., 1994, "A Loop-Closure Theory for the Analysis and Synthesis of Compliant Mechanisms," ASME J. Mech. Des., **118**, No. 1, pp. 121–125.
[8] Erdman, A. G., and Sandor, G. N., 1993, *Mechanism Design: Analysis and Synthesis, Vol. 1*, Prentice Hall, Inc., Englewood Cliffs, New Jersey.
[9] Midha, A., Norton, T. W., and Howell, L. L., 1994, "On the Nomenclature, Classification, and Abstractions of Complaint Mechanisms," ASME J. Mech. Des., **116**, No. 1, pp. 270–279.
[10] Ghali, A., and Neville, A. M., 1978, *Structural Analysis*, Chapman and Hall Ltd., London.
[11] Shoup, T. E., and McLarnan, C. W., 1971, "On the Use of the Undulating Elastica for the Analysis of Flexible Link Mechanisms," ASME J. Ind., **93**, Feb. pp. 263–267.
[12] Watson, L. T., and Wang, C. Y., 1981, "A Homotopy Method Applied to Elastica Problems," Int. J. Solids Struct., **17**, pp. 29–37.
[13] Stack, K. D., Benson, R. C., and Diehl, T., 1994, "The Inverse Elastica Problem and its Application to Media Handling," *Proceedings of the 1994 International Mechanical Engineering Congress and Exposition: Inverse Problems in Mechanics*, Proc. R. Soc. London, Ser. A, ASME, AMD-Vol **186**, pp. 31–36.
[14] Frisch-Fay, R., 1962, *Flexible Bars*, Butterworths, Washington.
[15] Banichuck, N. V., 1990, Chapter 7, *Introduction to Optimization of Structures*, Springer-Verlag, NY.